

absorptions have been observed in this region in other single-atom-bridged Fe(II, III) complexes,²⁴ but the lack of resolution of this band precludes detailed analysis.

Conclusions. Data obtained from a variety of physical methods demonstrate that the mixed-valence iron(II, III, III) acetates undergo dynamic intratrimer electron-transfer. With ⁵⁷Fe Mössbauer spectroscopy, rate constants for the intervalence transfer have been determined. Although the precision is not high, the barriers to thermal electron transfer have been extracted with use of an Arrhenius activation model. Recent theoretical work²⁵ has shown that many of the spectral properties of mixed-valence compounds are explicable in terms of a vibronic coupling model. For a symmetrical mixed-valence complex (such as is the case here) thermal intervalence-transfer should be a phonon-assisted process in which the ions are coupled by the asymmetric stretching vibrational mode of the interacting ions. It may prove possible to interpret the temperature dependence of the Mössbauer spectra with use of the vibronic coupling model for the electron-transfer process or with other models which consider tunnelling transitions explicitly. Such interpretations, however, must await more detailed theoretical and experimental examination.

These compounds have provided a unique opportunity to determine directly the energetics of thermal electron transfer. This thermal barrier has been determined in only one other molecular system.²⁶ Gagné and co-workers have used EPR measurements to estimate the electron-transfer rate, and thus the activation energy, in a binuclear copper(I, II) complex. Other compounds, such as the Creutz and Taube (C-T) complex [(NH₃)₅Ru-pyr-Ru(NH₃)₅]²⁺ (pyr = pyrazine), exhibit apparent²⁷ thermally activated electron transfer, but

experimental probes to measure the barrier directly are not available. Thus, although electron transfer is known to be fast at room temperature, on the time scale of ⁹⁹Ru Mössbauer spectroscopy (ca. 10⁻⁹ s) valences are trapped at 4 K.²⁸ The same types of information which we have obtained for the mixed-valence iron acetate are, in principle, obtainable from temperature-dependent ⁹⁹Ru Mössbauer spectroscopy. Unfortunately, low recoil-free fractions preclude the observation of ⁹⁹Ru Mössbauer spectra at temperatures where thermally activated electron transfer is facile.

The thermal barrier to electron transfer has been measured by using Mössbauer spectroscopy in other cases. With ¹⁵¹Eu Mössbauer spectroscopy, Eu₃S₄ has been shown to undergo intervalence electron hopping with an activation energy of 0.24 eV.²⁹ Electron hopping in this system, a continuous lattice semiconductor, can be correlated with the activation energy of 0.22 eV determined from electrical conductivity measurements. The semiconductor Sn₂S₃ has also been studied by variable-pressure ¹¹⁹Sn Mössbauer spectroscopy.³⁰ The results of this study are, however, more consistent with a "valence polarization" rather than true electron transfer in Sn₂S₃. Thus, Fe₃O(CH₃COO)₆(H₂O)₃ and its pyridine analogue provide a unique probe to the dynamics of electron transfer in molecular mixed-valence compounds and may consequently serve as important systems on which to focus efforts on fundamental understanding of the mixed-valence phenomenon.

Acknowledgment. This work was supported in part by the Office of Naval Research. We thank Dr. E. E. Weltin for helpful discussions.

Registry No. Fe^{II}Fe^{III}₂O(CH₃COO)₆(H₂O)₃, 36354-69-5; Fe^{II}-Fe^{III}₂O(CH₃COO)₆(C₃H₅N)₃, 35268-77-0.

Supplementary Material Available: Experimental and calculated magnetic susceptibilities (Tables I and II) and infrared spectral data and assignments (Tables V and VI) (6 pages). Ordering information is given on any current masthead page.

- (24) Walton, E. G.; Corvan, P. J.; Brown, D. B.; Day, P. *Inorg. Chem.* **1976**, *15*, 1737.
 (25) Piepho, S. B.; Krausz, E. R.; Schatz, P. N. *J. Am. Chem. Soc.* **1978**, *100*, 2996. Wong, K. Y.; Schatz, P. N.; Piepho, S. B. *Ibid.* **1979**, *101*, 2793.
 (26) Gagné, R. R.; Koval, C. A.; Smith, T. J.; Cimolino, M. C. *J. Am. Chem. Soc.* **1979**, *101*, 4571.
 (27) There is some controversy regarding this material, particularly with respect to a trapped vs. delocalized ground-state description. Arguments favoring a trapped (Class II) ground state are summarized in: Bunker, B. C.; Drago, R. S.; Hendrickson, D. N.; Richman, R. M.; Kessell, S. L. *J. Am. Chem. Soc.* **1978**, *100* 3805. Arguments favoring a delocalized (Class III) ground state are detailed in: Hush, N. S. "Mixed-Valence Compounds"; Brown, D. B., Ed.; Reidel: Dordrecht, The Netherlands, 1980; p 151.

- (28) Creutz, C.; Good, M. L.; Chandra, S. *Inorg. Nucl. Chem. Lett.* **1973**, *9*, 171.
 (29) Berkooz, O.; Malamud, M.; Shtrikman, S. *Solid State Commun.* **1968**, *6*, 185.
 (30) Amthauer, G.; Fenner, J.; Hafner, S.; Holzapfel, W. B.; Keller, R. *J. Chem. Phys.* **1979**, *70*, 4837.

Contribution from the Department of Chemistry, University of Vermont, Burlington, Vermont 05405

Reanalysis of the Thermal, Magnetic, and Spectral Properties of [Cr₃O(CH₃COO)₆(H₂O)₃]Cl·6H₂O on the Basis of an Intercluster Spin-Exchange Model

JAMES T. WROBLESKI, CHESTER T. DZIOBKOWSKI, and DAVID B. BROWN*

Received September 4, 1980

Inclusion in the Hamiltonian of a perturbing term which describes spin exchange between equilateral triangle clusters in [Cr₃O(CH₃COO)₆(H₂O)₃]Cl·6H₂O splits the ground state into two nondegenerate Kramers doublets. This splitting introduces a Schottky anomaly in the theoretical heat capacity curve. Two inequivalent pairs of trimer sites with different intercluster-exchange parameters are required to obtain agreement between experimental and theoretical heat capacities, low-temperature magnetic susceptibility data, and optical spectral data.

Previous theoretical models¹⁻⁶ proposed to account for the low-temperature thermal and magnetic susceptibility behavior

of [Cr₃O(CH₃COO)₆(H₂O)₃]Cl·6H₂O have been based on structural assumptions which are not substantiated by available data. These assumptions have been invoked because the

- (1) J. Wucher and H. M. Gijssman, *Physica (Amsterdam)*, **20**, 361 (1954).
 (2) J. Wucher and J. D. Wasscher, *Physica (Amsterdam)*, **20**, 721 (1954).
 (3) J. T. Schriempf and S. A. Friedberg, *J. Chem. Phys.*, **40**, 296, (1964).
 (4) N. Uryû and S. A. Friedberg, *Phys. Rev. A*, **140**, 1803 (1965).

- (5) M. Sorai, M. Tachiki, H. Suga, and S. Seki, *J. Phys. Soc. Jpn.*, **30**, 750 (1971).
 (6) M. Mishima and N. Uryû, *Phys. Lett. A*, **67**, 64 (1978).

thermal and magnetic data for this compound cannot be satisfactorily modeled without lifting the degeneracy of the two Kramers doublets which comprise the ground spin level. For example, even though the C_{2v} (isosceles triangle) model of Kambe which is given by eq 1, where S_1 , S_2 , and S_3 are spin

$$\mathcal{H} = J_0(S_1 \cdot S_2 + S_1 \cdot S_3) + J_1(S_2 \cdot S_3) \quad (1)$$

operators, describes the low-temperature heat capacity data for this compound, direct evidence for a structurally distorted Cr_3O cluster is not available. The room-temperature structure of this compound, as determined by single-crystal X-ray diffraction,⁷ consists of $[\text{Cr}_3\text{O}(\text{CH}_3\text{COO})_6(\text{H}_2\text{O})_3]^+$ ions in which the three chromium atoms are situated at the vertices of an equilateral triangle. The central O^{2-} is equidistant from and is in a plane with the chromium triangle. Furthermore, the model given by eq 1 cannot simultaneously describe the magnetic susceptibility and heat capacity data for this compound. Alternatively, Mishima and Urya⁶ have recently calculated the magnetic heat capacity for this material on the basis of the Dzyaloshinskii-Moriya exchange interaction given by eq 2. This "antisymmetric" exchange Hamiltonian splits

$$\mathcal{H} = \frac{iD}{2} \sum_{ij} (S_i^+ S_j^- - S_i^- S_j^+) \quad (2)$$

the ground state as required but fails to describe the magnetic heat capacity data of the chromium acetate complex. In actuality the Dzyaloshinskii-Moriya exchange interaction also requires a structurally distorted Cr_3O cluster in order that $|D| \neq 0$. Finally, Uryu and Friedberg⁴ have calculated the magnetic susceptibility and heat capacity partition functions derived from an axial crystal field model given by eq 3, where

$$\mathcal{H} = H_0 + \sum_{i=1}^3 D_i [(S_i^z)^2 - \frac{1}{3} S_i(S_i + 1)] \quad (3)$$

$H_0 = J_0(S_1 \cdot S_2 + S_2 \cdot S_3 + S_3 \cdot S_1)$. They also investigated the effect of inclusion in the Hamiltonian of higher spin coupling terms given by eq 4. Whereas eq 3 does not provide a sat-

$$\mathcal{H} = H_0 + J'[(S_1 \cdot S_2)(S_2 \cdot S_3) + (S_2 \cdot S_3)(S_3 \cdot S_1) + (S_3 \cdot S_1)(S_1 \cdot S_2)] \quad (4)$$

isfactory description of the thermal and magnetic data for the chromium acetate complex, eq 4 is Hermitian only if an additional term of the type

$$J''[(S_3 \cdot S_2)(S_2 \cdot S_1) + (S_1 \cdot S_3)(S_3 \cdot S_2) + (S_2 \cdot S_1)(S_1 \cdot S_3)]$$

is added to eq 4.⁸ The effect of this additional term is to restore the degeneracy of the two Kramers ground-state doublets.⁵

In view of the apparent failure of the above models to describe the properties of the chromium acetate trimer and because of our initial success in modeling the low-temperature magnetic susceptibility data for similar Fe(III) trimers⁹ with an intercluster spin-exchange model, we felt it would be appropriate to consider the possible applicability of such a model to the properties of the chromium compound. We took as our Hamiltonian eq 5, where S_A and S_B are spin operators which

$$\mathcal{H} = J_0(S_1 \cdot S_2 + S_2 \cdot S_3 + S_3 \cdot S_1) + j(S_A \cdot S_B) \quad (5)$$

couple cluster A with cluster B. Basis spin levels S_{iA} and S_{iB} were assumed to be the unperturbed spin vectors of the individual trimeric Cr_3O clusters. This analysis results in a 128-fold degenerate six spin problem. Although only the lowest few of the 30 spin levels which result from eq 5 con-

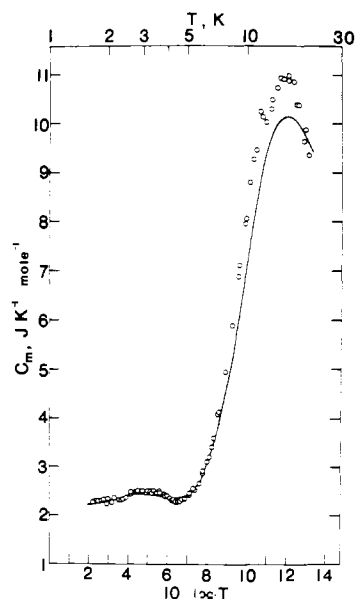


Figure 1. Experimental (O) and calculated (—) magnetic heat capacity of $[\text{Cr}_3\text{O}(\text{CH}_3\text{COO})_6(\text{H}_2\text{O})_3]\text{Cl}\cdot 6\text{H}_2\text{O}$.

tribute to the low-temperature limiting form of the appropriate partition function, we found it no less convenient to include all levels in the ensuing calculations.

Heat capacities for $[\text{Cr}_3\text{O}(\text{CH}_3\text{COO})_6(\text{H}_2\text{O})_3]\text{Cl}\cdot 6\text{H}_2\text{O}$ in the range 1.8–25 K obtained by Sorai et al. were fit to the appropriate partition function derived from the energies given by eq 5. The design and calibration of the calorimeters which were used to obtain these data have been published.¹⁰ The stated precision of the calibration measurements is $\leq \pm 3\%$ below 4 K and $\sim \pm 1\%$ above 4 K. These data constitute the most complete set of low-temperature heat capacities available for $[\text{Cr}_3\text{O}(\text{CH}_3\text{COO})_6(\text{H}_2\text{O})_3]\text{Cl}\cdot 6\text{H}_2\text{O}$.¹¹ These data were corrected for lattice heat contributions by using

$$C_V^D = 523.9718x_0^{-3} \int_0^{x_0} [x^4 e^x / (e^x - 1)^2] dx \quad (6)$$

for the Debye heat capacity, where $x_0 = 120/T$,² and

$$C_V^E = 54Ry_0^2 [e^{y_0} / (e^{y_0} - 1)^2] \quad (7)$$

for the Einstein heat capacity, where $y_0 = 270/T$ and R is the gas constant. The magnetic heat capacity, C_m , was obtained as

$$C_m(\text{obsd}) = C_p(\text{obsd}) - C_V^D - C_V^E \quad (8)$$

Experimental values of C_m obtained as above were fit to eq 5 by using the Simplex optimization algorithm.¹² Calculated and experimental values of C_m are shown in Figure 1. In order to adequately describe the low-temperature heat capacity data, it was necessary to consider the presence of two different equilateral Cr_3O trimer sites having distinct values of j . A distribution function of the type

$$C_m(\text{calcd}) = zC_m(J_0, j_1) + (1 - z)C_m(J_0, j_2) \quad (9)$$

was employed. Parameters $J_0 = -35k$, $j_1 = +0.9k$, $j_2 = +3.6k$, and $Z = 0.80$, where k is Boltzmann's constant, were obtained for the 1–6 K data of Sorai et al. The C_m curve calculated with these values is shown in Figure 1. In fitting these data

(10) M. Sorai, H. Suga, and S. Seki, *Bull. Chem. Soc. Jpn.*, **41**, 312 (1963).

(11) Wucher and Wasscher² reported heat capacity data above 4.2 K for this compound which disagree by approximately 40% with the data of Sorai et al.⁵ Because of the large experimental uncertainty of the former data, we have chosen to apply our model to the more extensive data of Sorai et al.

(12) S. N. Deming and S. L. Morgan, *Anal. Chem.*, **45**, 278A (1973), and references therein.

(7) S. C. Chang and G. A. Jeffrey, *Acta Crystallogr., Sect. B*, **B26**, 673 (1970).

(8) Quoted from ref 5 as a personal communication from Dr. P. Kisliuk.

(9) C. T. Dziobkowski, J. T. Wroblewski, and D. B. Brown, preceding papers in this issue.

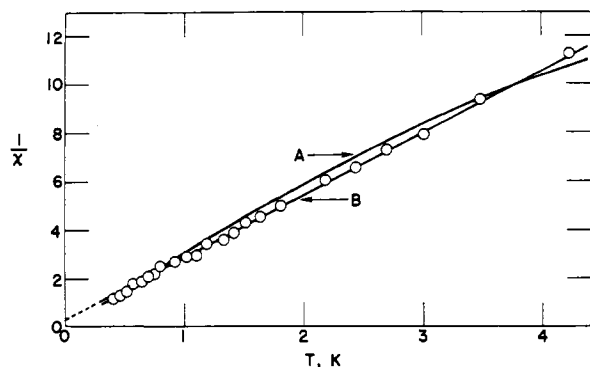


Figure 2. Reciprocal magnetic susceptibility vs. T .³ Smooth curve A represents the intercluster fit with parameters given in the text. Curve B represents the Curie-Weiss law fit with $C = 0.393$ and $\Theta = -0.13$ K.

it was our intention to model the 3 K Schottky-type anomaly as accurately as possible at the expense of not calculating the precise features of the 20 K maximum. Although the calculated maximum near 20 K exactly matches the experimental C_m maximum (Figure 1), we do observe a significant difference in their magnitudes. It is possible that this difference is a reflection of excess lattice heat contributions near this temperature.

For a test of the utility of these parameters, the magnetic susceptibility data of Schriempf and Friedberg³ for $[\text{Cr}_3\text{O}(\text{CH}_3\text{COO})_6(\text{H}_2\text{O})_3]\text{Cl}\cdot 6\text{H}_2\text{O}$ were modeled with parameters obtained from fitting the heat capacity data. Results of this calculation are shown in Figure 2. The experimental and calculated susceptibilities agree to within $\pm 3\%$, an accuracy within the quoted experimental uncertainty.³ Presumably the Curie-Weiss behavior of the susceptibility in the temperature range 0.4–4.2 K is attributable to the unique set of intercluster-exchange interactions present at low temperatures in this material. The possibility for such interactions has been stated previously.¹³

The mechanism for intercluster spin exchange is undoubtedly associated with the hydrogen bonding between trimer centers. The hydrogen-bonding network in crystals of $[\text{Cr}_3\text{O}(\text{CH}_3\text{COO})_6(\text{H}_2\text{O})_3]\text{Cl}\cdot 6\text{H}_2\text{O}$ involves carboxyl oxygens, lattice water molecules, and chloride ions.¹⁰ Because of the observed¹⁰ room-temperature disorder of the lattice water and halide sites, we would anticipate several possible types of intertrimer spin-exchange pathways in this material. It is, however, not possible to make an a priori statement about the number and magnitude of these pathways based on current data. A finite value of z however indicates that two or more intercluster-exchange pathways are available at low temperatures in this material.

Direct evidence for the presence of at least two sets of inequivalent trimer clusters in $[\text{Cr}_3\text{O}(\text{CH}_3\text{COO})_6(\text{H}_2\text{O})_3]\text{Cl}\cdot 6\text{H}_2\text{O}$ at low temperatures has been presented by Ferguson and Güdel.¹⁴ These investigators obtained the absorption-emission spectrum of the complex and completed an analysis of the spectrum by assuming two sets of trimer clusters. This analysis was taken¹⁴ to support the earlier suggestion made

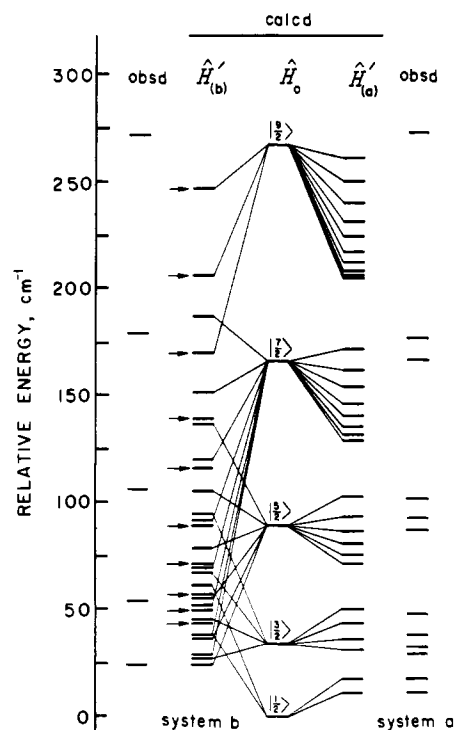


Figure 3. Comparison of calculated and experimental spin level energies for the trimer systems of Ferguson and Güdel.¹⁴ Spin levels marked with an arrow arise from the unperturbed $|^9/2\rangle$ trimer state.

by Sorai et al.⁵ that two sets of isosceles trimers were present in the unit cell at low temperatures. We have undertaken a reanalysis of this spectrum on the basis of our intercluster Hamiltonian (eq 5). A comparison of calculated and experimental spin levels is illustrated in Figure 3. Calculated energies on the right of this figure were obtained by using eq 5 with $J_0 = -35k$ and $j_1 = 0.9k$ whereas energies on the left refer to eq 5 with $J_0 = -35k$ and $j_2 = 3.5k$. We believe that the former spin levels correspond to trimer system a of Ferguson and Güdel.¹⁴ Our analysis of the heat capacity data shows that this system comprises 80% of the total number of trimers and, therefore, should correspond to the most intense absorptions in the optical spectrum as observed by Ferguson and Güdel. Agreement between calculated and observed spin level energies is excellent for the manifold of $|^1/2\rangle$, $|^3/2\rangle$, and $|^5/2\rangle$ states in system a. Our analysis of the spin system with $j_2 = 3.5k$ indicates that a spin level which originates from the unperturbed $|^5/2\rangle$ excited state lies lowest. We believe that this spin system corresponds to trimer set b of Ferguson and Güdel and that the large intercluster splittings very much complicate analysis of the spectrum of this set of trimers. Observed energy levels¹⁴ are shown on the extreme left of Figure 3. However, correlation with calculated spin levels is uncertain.

We believe that the intercluster model proposed above provides a physically realistic basis for understanding the properties of numerous similar cluster compounds. We propose that such a model be applied as a perturbation to the normal Heisenberg spin-exchange model in those cases in which models such as eq 1–4 are not substantiated by direct physical measurements.

Registry No. $[\text{Cr}_3\text{O}(\text{CH}_3\text{COO})_6(\text{H}_2\text{O})_3]\text{Cl}$, 35268-73-6.

(13) F. E. Mabbs and D. J. Machin, "Magnetism and Transition Metal Complexes", Chapman and Hall, London, 1973, p 194.

(14) J. Ferguson and H. U. Güdel, *Chem. Phys. Lett.*, **17**, 547 (1972).